Egypt. J. Geo. **Vol. 65,** pp: 105-122 (2021)

Egyptian Journal of Geology
https://egjg.journals.ekb.eg

Zeolite Crystal Growth Generations During Diagenetic and Hydrothermal Processes- Case Study of Lacustrine Volcaniclastics, Abu Treifiya Area, Cairo-Suez Road, Egypt

Kabesh, Mona and **Shallaly, Nahla A.**
Geology Department, Faculty of Science, Cairo University, Egypt

ZEOLITES and clay minerals are common authigenic minerals in volcano-sedimentary rock association in the Abu Treifiya basin. They are formed by hydrolysis alteration of basic volcanic glass by reaction with percolating water in a partly closed basin of saline-alkaline lacustrine environment. The zeolites and associated clay minerals and calcite are studied and described in detail microscopically and by X-ray diffraction, also occasionally scanning electron microprobe and Raman techniques are applied. The zeolite mineral species of phillipsite, thomsonite, tobermorite, chabazite, natrolite and analcime are recorded and described. Palagonitization and alteration of volcanic glass result in three stages of authigenic mineral formation; 1) clay minerals as smectite, chlorite/smectite (mixed layer) and chlorite, 2) zeolite minerals, and 3) finally calcite. These associations are found to form in two paragenetic phases: A) diagenetic phase, represented by clay minerals, followed by phillipsite or thomsonite that may be overgrown by phillipsite, filling interstitial spaces, vesicles and amygdales in mostly all facies types of the volcano-sedimentary succession. These resulted from volcanic glass alteration during increasing pH, alkalinity and salinity of the environment. Analcime granular crystals form in lapilli tuff and hyaloclastite tuff in higher Na rich saline -alkaline environment at extreme palagonitization, and B) hydrothermal phase represented by open space filling of cross cutting fractures and/or manifested by formation of tobermorite spherules along basalt lacustrine carbonate contacts. Large vugs exhibit sequential crystallization of Ca zeolite thomsonite spherules followed by calc- sodic zeolite Ca- chabazite; with decreasing temperature and increase in Na in the fluid Na rich fibrous natrolite crystallize. Hydrothermal veins are filled by large euhedral Na- chabazite associated with chalcedony, Fe- oxyhydroxides and clays.

Keywords: Zeolites, palagonite, lacustrine, volcaniclastics, diagenetic crystallization, hydrothermal, Abu Treifiya.

Introduction

Oligo- Miocene Red-Sea rift volcanics in Egypt are manifested by basaltic dykes, sills and flows that are occasionally accompanied by thin volcaniclastic beds (El- Bayoumi, *et al*., 1998; Farahat, *et al*., 2007; Shallaly, *et al*., 2013; Khalaf and Sano, 2020). In the Abu Treifiya basin located along the Cairo–Suez Road, north Eastern Desert, Egypt (Fig.1a), the volcaniclastics/flows ratio is surprisingly higher than any other locality. Few researches on these volcanics were carried out, that dealt with the mineralogy and geochemistry (*e.g.* Abou Seda, 1980 and 2005), and the contact effect of the dolerite dykes on the limestone (El Sharkawi and Abu Khadra, 1968), the lacustrine volcano-sedimentary succession (Abdel-Motelib, *et al*., 2015) and finally the structure and peperite formation of these rocks with the surrounding sediments (Khalaf, *et al*., 2015). The previous

Correponding author: Kabesh, Mona, Email: monakabesh@yahoo.com
Accepted: 04/11/2021; Received: 07/12/2021
DOI: 10.21608/egjg.2021.106000.1013

studies mentioned the presence of zeolites without detailed description of their mode of occurrence, mode of formation and paragenetic sequence

The recognition of zeolites in the altered volcaniclastic units associated with the Oligo-Miocene rift related basalt flows and dykes in Abu Treifiya area was a catching sight motivating detailed investigation. The current research focuses on the process of zeolitization of the volcano-sedimentary succession in this area, identifying and describing the zeolites paragenesis, crystallization sequence and mechanisms of formation. The present study aims to shed light on the zeolites in this area to be a building unit for further future detailed investigations and evaluation for assessing its economic potentiality concerning their distribution, extension, minability, and means of beneficiation.

Zeolites are crystalline aluminosilicates with periodic arrangement of cages and channels which were found to have extensive industrial uses as catalyst, adsorbent, and ion exchange (Pansini, 1996; Ming, and Allen, 2001; Mormone, 2020). They are generally formed by different processes due to the interaction of aqueous fluids with silicic to mafic volcaniclastics, in various geological environments, that range from diagenesis in marine open hydrologic system (Sheppard and Hay, 2001; Hay and Sheppard, 2001) or closed saline alkaline lakes, and fresh water hydrologic systems (Surdam,1977; Langella et al., 2001). Also, through low temperature hydrothermal (Gottardi, 1989; Utada, 2001; Triana et al., 2012; Bastias , 2016), pegmatitic (Orlandi and Scortecci, 1985) to burial metamorphic environments (Neuhoff et al., 1999) and geothermal environments (Weisenberger and Selbekk, 2008). The most common zeolite occurrences are related to Tertiary-Quaternary volcanic fields, as they are related to the palagonitazation process of the metastable volcanic glass that is not preserved in rocks older than mid-Tertiary (Risso et al., 2008). Palagonitization of volcanic glass is ascribed to glass hydrolysis, formation and evolution of palagonite followed by crystallization of authigenic minerals such as smectite, zeolites and calcite, (Thorseth et al., 1991; Crovisier et al., 1992; Stornick and Schminke, 2001 & 2002). Such a process involves the leaching of certain elements such as Si, Ca, Na and K and gain of H_2O, Fe and Ti.

Geological Setup

The eastern and southern foothills of the uplifted Eocene limestone block of Gebel Abu Treifiya, Cairo-Suez Road (Fig. 1a and b), are occupied by four phases of Oligo-Miocene basaltic flows and dykes and volcaniclastic rocks (Abou Khadra et al., 1993; Abou Seda, 2005). The volcaniclastic sequence represents water-laid deposits with discontinuous intermittent gently dipping beds of repeated fining-upward cycles reflecting fluctuations of wet and dry conditions under fluvial to saline-alkaline lacustrine environment (Abdel- Motelib et al., 2015). Khalaf et al. (2015) argued that the Abu Treifiya basin represents an E–W-trending pull-apart extensional basin, along which the rocks are tilted, and faulted with cataclastic deformation. The E–W and NW- to WNW trending normal faults with displacement down to the SW, resulted in juxtaposition of the pre-rift Eocene carbonate units against the Oligo-Miocene syn-rift basaltic units. They discussed the dynamic basaltic lava-sediment interaction and the formation of peperite. Doleritic dykes intruded the Eocene limestones and produced a metasomatic hybrid zone with formation of wollastonite marble along their contacts (El Sharkawi and Abu Khadra, 1968).

The present field investigation revealed that the volcaniclastic rocks form multiple lava fragment-rich surge units interspersed with lapilli-tuff layers, hyaloclastites, vitric tuff and tephra beds that have been altered to clays and zeolites (Fig. 1c). They range from clast-to matrix-support fabrics and are capped by basaltic flows with conspicuous columnar jointing (Fig. 2a). They exhibit some depositional sedimentary features as graded bedding, flaser-bedding and scour and fill structures suggesting a phreatomagmatic depositional environment of the explosive surges. The graded bedding is best recorded in the lapilli tuff, which forms ca 2m thick of well sorted and partially welded lapilli-rich layers. The beds are composed of spherical coarse-lapilli grading upwards to beds of finer-lapilli size (Fig. 2b).The hyaloclastites are subdivided according to their sizes into hyaloclastite breccias with bomb to coarse lapilli sized clasts and tuffs with lapilli to ash- sized clasts also arranged in graded bedding pattern. Tens of centimeter thick achnelithic tephra beds are recorded, occasionally in association with the hyaloclastites. They exhibit a coarsening-upward pattern and are composed of ash- to lapilli-sized achnelith (Fig. 2c). These tephra deposits may be subaerial similar to that associated with

fire fountain scoria in Strombolian and Hawaiian style volcanism, or of hydrovolcanic explosion origin of Cannata, *et al*. (2012) and Carracedo-Sánchez et al. (2016). The volcaniclastic sequences are often overlain by fluvial sandstones and lacustrine carbonates. The lacustrine carbonates are lenticular in shape, nodular, bioturbated, and in situ brecciated. The basaltic flow lower boundaries mix with these rock facies, forming a characteristic peperite zone (Fig. 1c).

The Abu Treifiya zeolite mineral association is best recorded along Wadi Kiheiliya and Umm Thibua volcaniclastics (Figs. 1b & c). They occurs either as diagenetic mineral association in the host volcaniclastics or as hydrothermal open space-filling of cavities and fractures of the volcaniclastics, basaltic flow and lacustrine limestone.

Sampling and Analytical Techniques

A total number of 24 representative samples were collected from the volcaniclastic rock units and the associated carbonates, infilled veins and vugs. These are in thoroughly investigated under the reflected microscope highlighting on the zeolite crystal growths and textures. Nine selected samples were analyzed by X-ray diffraction (XRD) technique of bulk samples and clay mineral analysis of the < 2 μm sub-fraction. Additionally, zeolites and clay minerals were identified by scanning electron microscopy (SEM) and Raman techniques. The XRD and SEM techniques were carried out in the Egyptian Central Metallurgical R & D Institute; the Raman technique was performed at the Faculty of Nanotechnology, Cairo University.

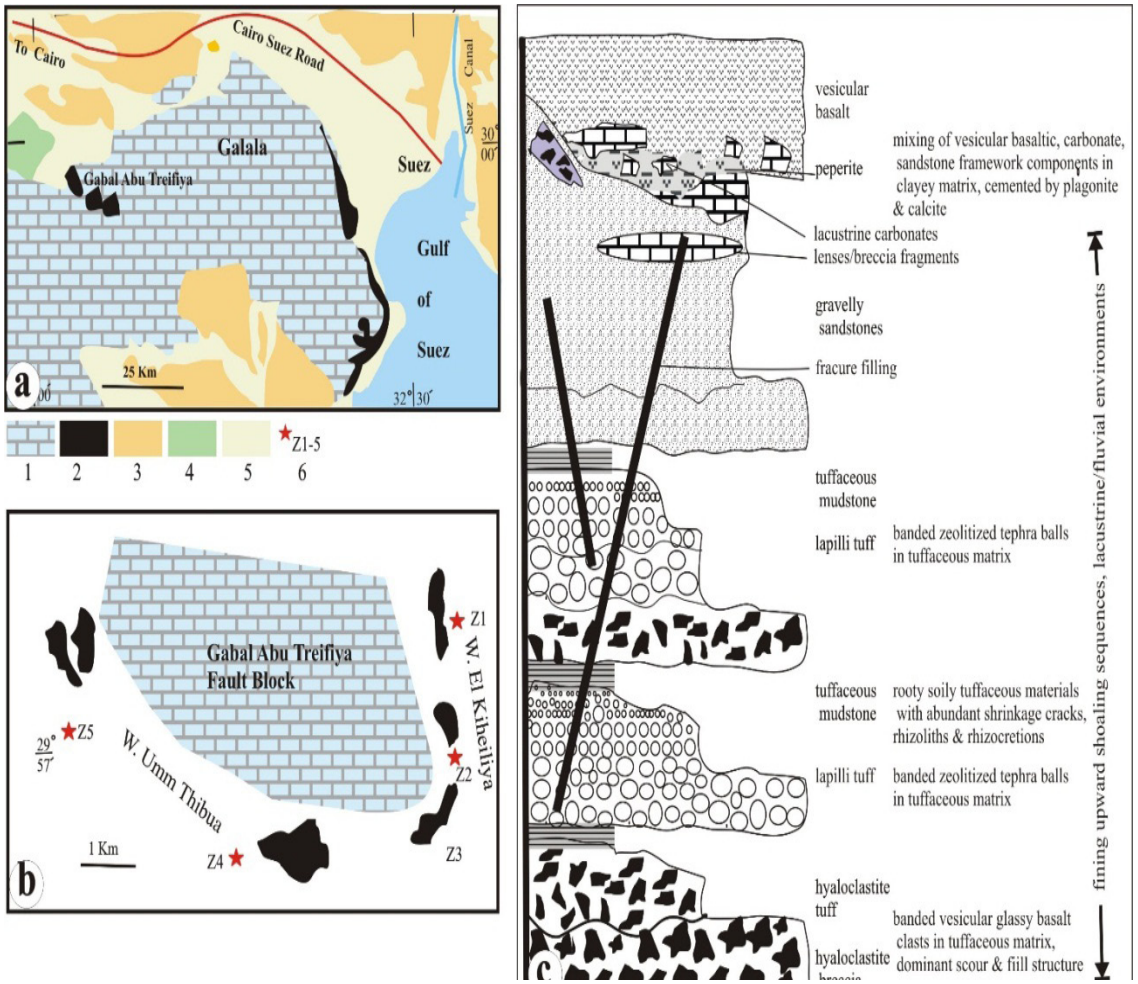

Fig. 1. a. A simplified geologic map (after Said, 1990), showing the location of the Abu Treifiya basaltic occurrence. 1: Eocene limestone, 2: Basaltic rocks 3: Miocene 4: Pleistocene and Recent clastics. b. Sketch drawing showing the distribution of basaltic exposures (Z1-Z5) of W. El Kiheiliya and W. Umm Thibua (after Abu Seda, 1980 and Abdel Motlib et al., 2015). c. Representative sketch vertical profile of the fining upward basaltic volcaniclastics and lava flows at the entrance of W. El Kiheiliya, not to scale.

Results

Host rock petrography

Coherent lava flow

They range from scoraicous, hypocrystalline to holocrystalline, amygdaloidal plagioclase - pyroxene-olivine phyric basalts. The plagioclase forms slightly altered microphenocrysts, small laths and minute varioles that are embedded in the glassy mesostasis. Pyroxene forms scattered augite/pigeonite glomerophenocrysts or small anhedral grains specifically in the ground mass of the holocrystalline basalts. Olivine is recorded as microphenocrysts accompanying pyroxene. Vesicles are variably sized, irregular, rounded to elliptical (Fig. 2d); they may reach up to 40% of the rock by volume (in scoriaceous variety).These rocks experience different degrees of hydrothermal alteration that include devitrification of glass, replacement of primary minerals filling voids and vesicles by secondary components. The primary minerals exhibit different degrees of alteration where plagioclase and pyroxene are slightly altered and replaced if any by calcite. Conversely, olivine is rarely recorded fresh; it is always pseudomorphed by smectite and less commonly by serpentine and iddingsite.

Lapilli tuff

The framework of this lithofacies consists of numerous, light-colored, rounded to ovoidal zeolitized clasts (tephra balls) coated by rims of fine ash and mud. The tephra balls are of uniform size (0.04-1cm) set in a fine vitric tuffaceous matrix with variable amounts of fine-grained zeolites, and smectite. The clasts are composed of severely zeolitized vitric tephra with numerous plagioclase laths, giving them their light color (Fig. 2e). Additionally, minute rounded zeolitized glassy fragments that are surrounded by a palagonite rim (Fig. 2f), larger elongated palagonite remnants, crystal fragments of pyroxene, zeolitized plagioclase and less commonly severely altered olivine are dispersed in a fine matrix of ash and cemented by clays, analcime and fine calcite.

Hyaloclastite breccia

This poorly sorted and matrix-supported rock composed of variably sized basaltic fragments embedded in a fine-grained matrix. The fragments are of two types: angular, non-vesicular olivine-augite- plagioclase- phyric tachylitic basalts with size range 0.5-10mm. Olivine is pseudomorph by a mixture of serpentine, smectite and vermiculite. Less abundant curvilinear clasts (1 – 15 mm in size) of pigeonite-plagioclase phyric scoriaceous basalts are recorded (Fig.2g). The amygdales are small, irregular to rounded and lined with zeolites and cored by smectite and chlorite/smectite (corrensite). The tuffaceous matrix is fine-grained and consists of a mixture of chlorite, smectite and zeolites (phillipsite) and glass relics. Small crystal fragments of quartz set in the matrix and are surrounded by a veneer of sideromelane. The lack of proper jigsaw fit is attributed to the alteration of the glass into the authigenic minerals. Moreover, the presence of two types of basaltic clasts and quartz grains indicate that these hyaloclastites are of resedimented rather than of in situ types. Continuous movement of the internal lava, flowing over steep slopes, magma intrusions into the hyaloclastite, or seismic activity can all cause "*resedimented hyaloclastite"* to be formed (McPhie et al., 1993). In the rift-related Abu Treifiya basin the seismic activities are the most plausible explanation for the formation of the recorded "*resedimented hyaloclastite"*.

Hyaloclastite tuffs

This rock is fine-grained composed of lithic and crystal fragments, and glassy shards set in a fine-grained tuffaceous matrix. The lithic fragments are similar to but finer (0.5-2mm) than that described in the hyaloclastite breccia. This unit is characterized by the presence of variably sized and elongated palagonitized achneliths, corresponding to type two of Carracedo-Sánchez et al. (2016). They are characterized by hyalocrystalline texture with light brown and highly vesicular glassy mesostasis (sideromelane) and cored by plagioclase or olivine phenocrysts (Fig. 2h). The crystal and crystal fragments are partially zeolitized plagioclase, olivine pseudomorphs and slightly calcitized pyroxene.

Peperites

These deposits form a hybrid zone along the volcanic - sedimentary contact due to mixing of fluvial sandstone or lacustrine carbonates with the syn-sedimentary volcanic materials. The sandstone is arenitic in composition, fine grained (0.1-2mm) and moderately sorted. Quartz forms 0.1-0.5 mm long, angular to subangular, equant to elongated and fractured grains. Angular lithic fragments of plagioclase-pyroxene phyric scoriaceous basalts are dispersed between the quartz grains, these fragments are surrounded by a palagonite rind that reflects the presence of a former chilled margin of these clasts (Fig. 3a). Small rounded yellowish brown banded

palagonite clasts are also recorded between the quartz grains. These components are cemented by a palagonite network, calcite, and a mixture of clay minerals. The lacustrine limestone is matrix-supported with framework components of Eocene fossiliferous limestones and bioclasts that are embedded in a fine-grained, micritic matrix. The recorded fossils and fossil fragments were identified as Dictyoconus Egyptiensis (a large benthic Foraminifera) with echinoid test fragments and bivalve shell fragments (ghost structure) that belong to the Middle Eocene shallow marine environment (Kassab, personal communication). Differently sized fragments of scoriaceous basalts are recorded within the lacustrine limestone. These fragments exhibit chilled margins with the development of very thin recrystallized calcite crystals around the fragments (Fig. 3b).

Tuffaceous mudstone

This unit is variably colored, massive and very fine-grained that is composed of a combination of vermiculite, montmorillonite, chlorite and calcite with minute quartz grains. The observed color variation is attributed to high concentrations of chlorite, Fe oxyhydroxides or carbonaceous organic matter. Additionally, the presence of small subangular clasts of plagioclase-phyric tachylitic and scoriaceous basalts suggest reworking of these sediments. Gypsum veins with antiaxial fibrous texture exhibiting a median zone and two oppositely directed fibrous zones, where the long straight to slightly curved gypsum fibers are normal to the vein walls are observed. These veins may host minute fragments of the country rocks and the basalts (Fig. 3c). The presence of desiccation cracks together with rhyzocressions and rhyzoliths suggest that these mudstones were subjected to pedegenic processes as discussed by Abdel Motlib et al. (2015).

Authigenic minerals

The succession of volcaniclastic units have been strongly altered, resulting in the formation of authigenic minerals, mainly zeolites, clay minerals and calcite. Detailed textural and mineralogical features of secondary minerals observed in intergranular spaces, amygdales, vugs and veins suggest two main stages of zeolite crystallization: A) diagenetic stage and B) hydrothermal stage. Each stage exhibits its unique macroscopic characteristics, microscopic textures and zeolite mineral assemblage and paragenetic sequence.

Diagenetic mineral assemblage

Shortly after deposition of the volcanogenic sediments in an aqueous environment, started the diagenetic processes as post- depositional changes of the deposits. Diagenesis starts by circulation of pore fluids in the unconsolidated deposits. At the early diagenesis, basaltic glass is rapidly altered by percolating fluids at low temperatures (<100^{o}C) forming palagonite. Hydrolysis alteration of palagonite led to the precipitation of authigenic minerals, successively as 1) clay minerals, 2) zeolites, and 3) calcite. Crystallization starts in primary pore spaces on rims of minerals, glassy basaltic clasts, and internal vesicle walls with a coating of smectite followed by zeolite and calcite cements until almost all spaces are filled. The presence of all secondary minerals including the different zeolite species are confirmed by the XRD, SEM and Raman techniques.

Palagonite

All the studied rocks contain volcanic glass in different proportions and degrees of alterations. The most common form is fresh tachylite that is recorded in the groundmass or along the walls of the vesicles in the coherent lava flow (Fig. 3d) or as rock fragments in the volcaniclastic rocks. Fresh sideromelane is recorded as thin veneers around quartz clasts in hyaloclastite breccia or as elongated achnelithic fragments in the hyaloclastite tuffs, that show partial alteration to palagonite (Fig. 2h). Palagonite is a common alteration product of sideromelane as a consequence of hydration. It is observed as yellowish brown to pale brown gel material forming vesicular clasts of different shapes and sizes, lining vesicles (Fig. 3e) or at the margins of glass clasts and shards in all types of volcaniclastic rocks. Palagonite may exhibit banding with much darker rims reflecting variation in chemical composition and display thermal contraction fractures (Fig. 3f). It is mainly found as gel palagonite that transforms to fibrous palagonite (Fig. 3g). Palagonitization process could be partially ascribed to biogenic action as the current study recorded the presence of some bacterial filaments adhere to the growing smectite (Fig. 3e). The biogenic alteration of glass was reported earlier by Abdel-Motelib & Kabesh (2015).

Clay minerals

Clay minerals can be distinguished as smectite, mixed-layer clays (chlorite/ smectite), chlorite, vermiculite and less common kaolinite and illite, based on their optical characteristics and X- ray diffraction patterns.

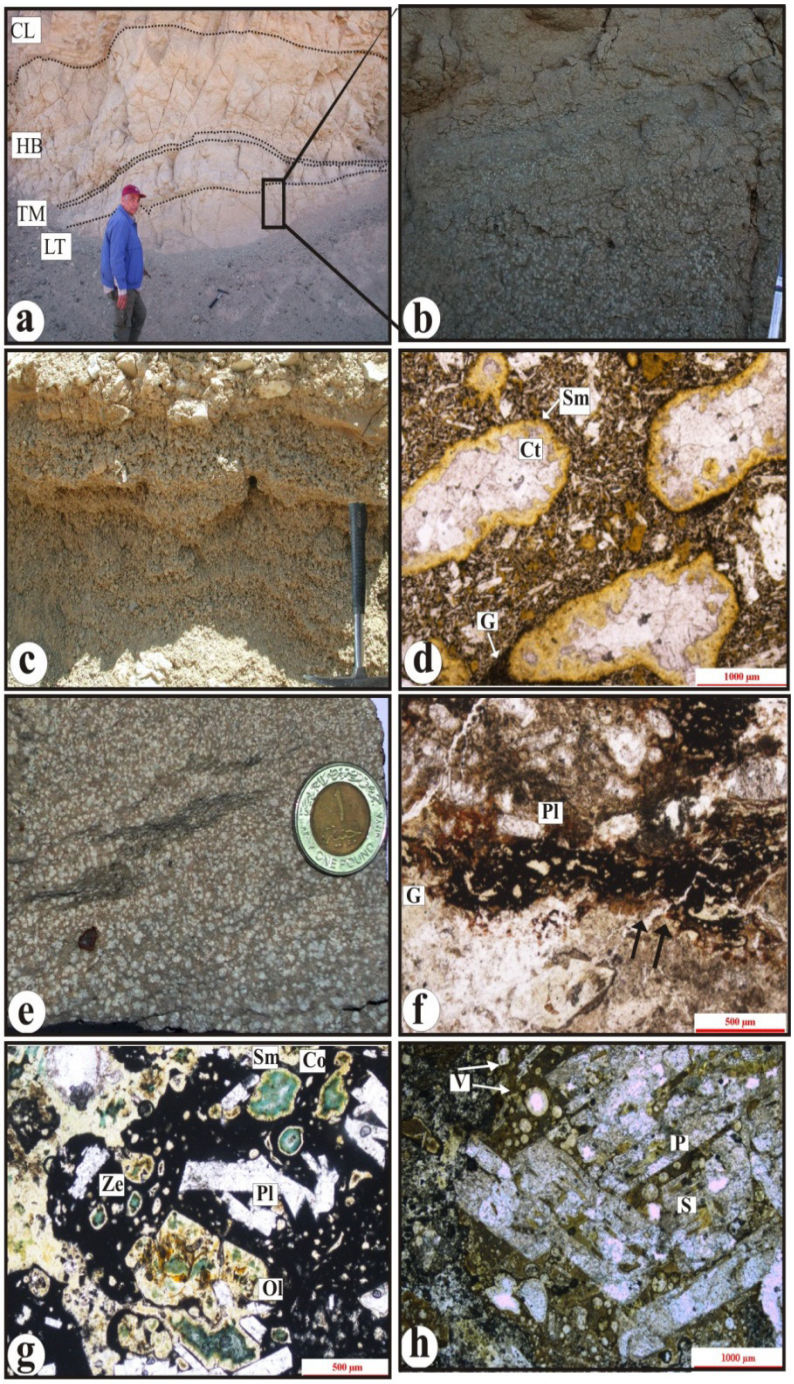

Fig. 2. a. A section of volcaniclastics with a basal lapilli tuff layer (LT), followed by a thin tuffaceous mud (TM), hyaloclastite breccia (HB) and topped by a coherent lava flow (CL). b. A close-up view of the lapilli tuff layer showing conspicuous fining upward graded bedding. c. a general view of the achnelithic tephra layer d. Elongated and parallel vesicles that are filled with calcite (Ct) and rimmed by yellowish smectite (Sm), note the presence of glassy (G) chilled margin along the outer rim of some vesicles. Scoriaceous olivine basalt, PP. e. A hand sample showing variably sized zeolitized tephra balls in lapilli tuff. f. An elongated vesicular tachylitic fragment (G) that is rimmed by brown palagonite (arrows) that form small rounded clasts as well in tuffaceous matrix with slightly zeolitized plagioclase crystal fragments (Pl). g. Vesicular tachylitic olivine (Ol) plagioclase (Pl) phyric basalt clasts that are separated from each other by a mixture of clay minerals, note the sequential growth of yellowish smectite (Sm)- colorless zeolite (Ze)- bluish green corrensite(Co) in the clast vesicles, hyaloclastite breccia, PP. h. A plagioclase phenocryst-cored achneliths that composed of brown palagonite (P) with numerous smectite-lined rounded vesicles (V), note the presence of buff sideromelane (S) relics in between the plagioclase in tuffaceous matrix, PP.

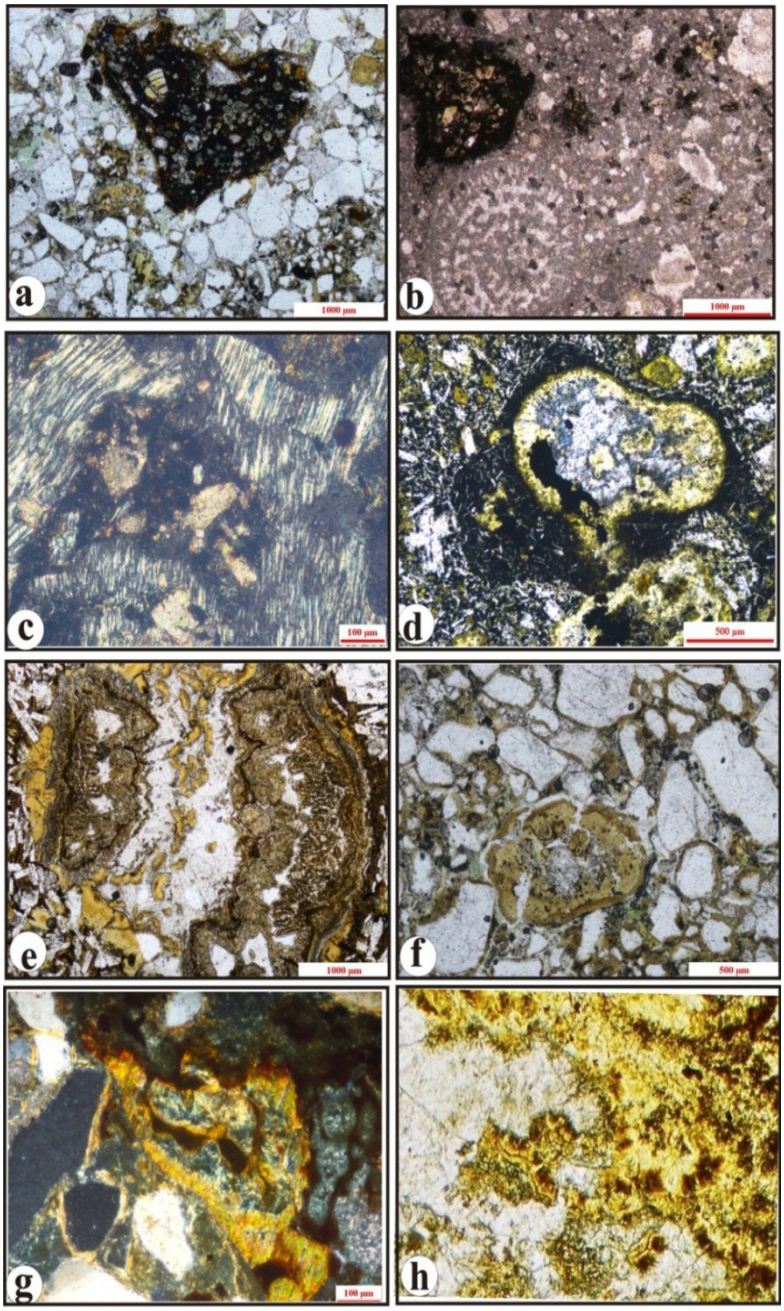

Fig. 3. a. A scoriaceous basalt clast that is rimmed by reddish brown palagonite rind in between quartz grains in sandstone-hosted pepertite, PP. b. Lacustrine limestone peperite showing scoriaceous basalt clasts with black chilled margin indicating syn-sedimentary eruption, note the presence of reworked clasts of older limestone and large Foraminifera at the lower part of the photo, PP. c. Antiaxial gypsum vein nucleated around a vesicular glassy basalt in tuffaceous mudstone. D. A pillow-like amygdule with zonal arrangement of smectite-zeolite-calcite, it is surrounded by and control the shape of a chilled margin, PP. e. Large spherical amygdales of an overall crustified comb texture, are lined with a brown veneer of palagonite, a yellow rind of smectite, then a thick layer of brownish dolomite rimmed by a dark brown Fe-oxide thin band. The vesicles are cored by calcite, with relicts of smectite. Amygdaloidal olivine basalts, PP. f. Cracked vesicule-rich, rounded clasts of banded palagonite cored by calcite are dispersed between the quartz grains, sandstone-peperite. g. A glassy shard replaced by a sequence of orange gel then fibrous palagonite, followed by greenish smectite then an outer rim of brown mica, note the presence of an interconnected palagonite network around the quartz grains, Sandstone-peperite. h. Brown gel palagonite remnants in a yellow banded palagonite and later smectite, note the presence of bacterial filaments (arrows).

Smectite is precipitated in the early diagenetic stage by alteration of palagonite along the outer rims of glassy basaltic clasts and glass shards and lining the inner walls of vesicles, also filling pore spaces. Smectite forms a yellowish to pale brownish aggregate of tiny flakes (Figs. 2d, 3e & g). Mixed-layer clays (MLC) mostly as chlorite/ smectite mixed layer type (corrensite) are observed in the hyaloclastite breccias and tuffs and the amygdaloidal olivine basalts. They show pronounced pleochroism of light to darker green colors as coarser radiating bundles, sometimes associated with zeolite crystals. They are found in voids and lining vesicles commonly precipitate following smectite. Some vesicles are filled by chlorite / smectite mixed layer clays in which the increase in chlorite content is observed from the outer wall inwards (Fig. 2g).

Chlorite is generally seen as greenish void fillings in rocks with corrensite. Vermiculite is observed in the olivine basalts from alteration of olivine crystals sometimes accompanying serpentine as pseudomorph after olivine. Vermiculite is also detected in the tuffaceous mudstone due to argillitization. The XRD patterns of the hyaloclastite breccias, tuffs and lapilli tuffs show smectite, chlorite/smectite (corrensite), chlorite, vermiculite-chlorite mixed layers and traces of illite (Fig. 4). The strong reflection at 15.2Å accompanied with ~7.34 Å peak represents the corrensite whose peak positions are indicative of ~58% chlorite. A basal smectite reflection observed at 16.5 Å indicative of some 18% chlorite layers. Heat treatment reduced peaks to 13.8Å and ~12.7Å. Illite is recognized by the 10 Å and 5 Å reflection peaks. In these samples 14 Å peak of chlorite is observed after heat treatment but is smaller than the 10 Å peak suggesting that vermiculite or a mixed chlorite- vermiculite may be present.

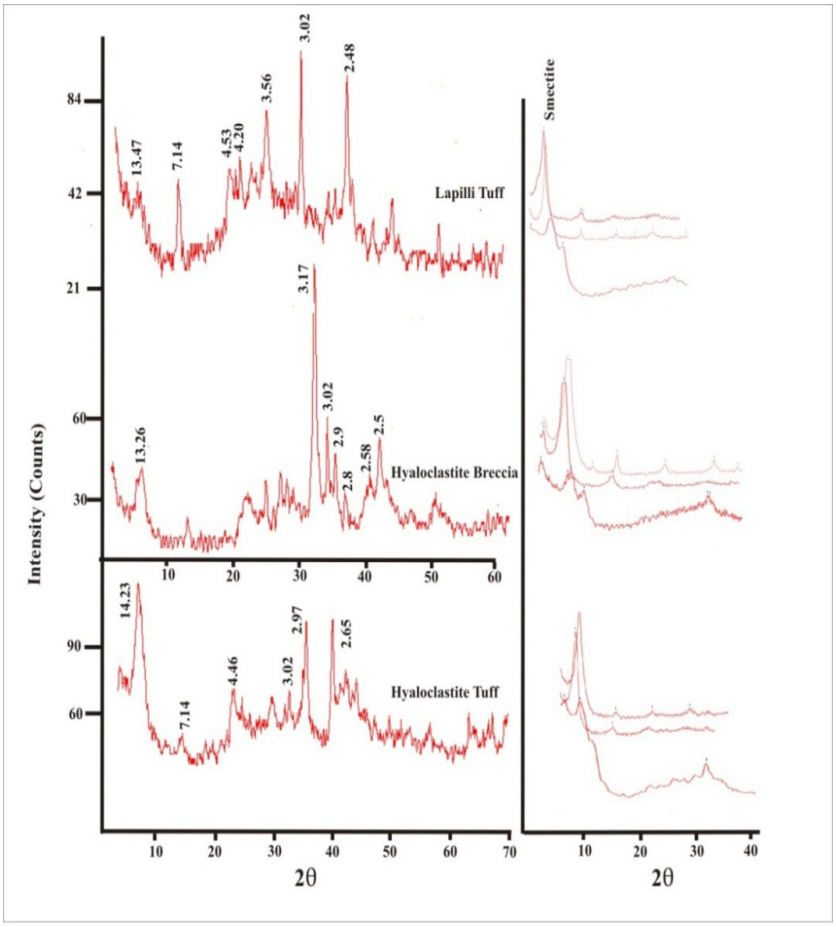

Fig. 4. XRD patterns of bulk composition and clay fraction of lapilli tuff, hyaloclastite breccia and tuff.

Zeolite generations

Zeolites crystallized in the late diagenetic stage as pore-space filling or replacement of primary components such as volcanic glass and plagioclase. The interstitial spaces in volcaniclastics lined earlier by a coat of smectite commonly show overgrowth by fine-grained fibrous aggregates of phillipsite and thomsonite in the tuffaceous matrix of the hyaloclastite breccia and tuffs, respectively (Fig. 5a) or thomsonite followed by phillipsite (Fig. 5b). Phillipsite fibers ṯrim basaltic glass clasts and crystal fragments. In the hyaloclastite tuff, the amygdales of glassy clasts are filled with about 30-50μm long, creamy bladed crystal aggregates of phillipsite, (Fig. 5c). Such rhythmic pattern of crystallization of thomsonite and phillipsite radiating fibers with idiomorphic terminations towards pore spaces, followed by filling with blocky calcite resemble the diagenetic crystallization rhythmites (DCRs) described by Fontbotẽ and Amstutz (1980) and El Aref (1984).

The tephra balls in the lapilli tuff are highly zeolitized with the formation of phillipsite, the tuffaceous matrix is severely altered to a mixture of zeolites (e.g., thomsonite and phillipsite), smectite and calcite with relics of glass. Furthermore, in the hyaloclastite breccia and tuffs and the lapilli tuff, large, rounded crystals of analcime are recorded in their tuffaceous matrix. They are up to 0.4-1.2 mm in size, isotropic and usually rimmed and invaded by late calcite (Fig.5d). The presence of such diagenetic analcime was confirmed by the Raman technique (Figs. 5e & f). They are also observed as alteration of primary minerals, volcanic glass, and tephra balls. Zeolitization of plagioclase is common where zeolites alone (Fig. 5a) or combined with calcite replace plagioclase. Thomsonite and calcite pseudomorphs of plagioclase micro-phenocrysts and groundmass crystal fragments are common in hyaloclastite breccias and tuffs. In the volcaniclastic rocks, alteration is patchy or dominical depending on the distribution of the glassy shards and clasts. In coherent rocks, specifically those with glassy mesostasis, the groundmass is composed of variable proportions of zeolites- sideromelane / tachylite -smectite - chlorite surrounding the primary minerals.

Calcite

It is the last of the authigenic minerals to crystallize. It is found as late cement filling the intergranular spaces or cavities and pore spaces, in the form of blocky mosaic crystals or crustified layers. Calcite in large, rounded cavities may include reddish brown segregation of Fe oxyhydroxides globules, thin bands and semicircular rings of concentric botryoidal structure.

Hydrothermal mineral assemblage

Later zeolite crystallization that is attributed to a hydrothermal generation exhibits an open space filling mechanism with different patterns. They range from infilling of amygdales in basalts to corrosion vugs and cross cutting fracture vein filling. Amygdales in basalts are the most abundant open space filling features; they range from rounded to irregular amygdales about 1mm to large rounded vugs. They are fully filled with zeolites or associated with other minerals. Fully filled zeolite rounded amygdales with a diameter 0.2-1.5mm are recorded in the scoriaceous basalts at contact with lacustrine limestone blocks. They are lined by a thin rim of about 50μm long fibrous crystals of chlorite, then filled by flower-like radiating 100-250 μm long fibrous and variably directed aggregates of tobermorite (Figs. 5 g & h). Some large amygdales in the amygdaloidal basalts exhibit crustiform banded infill with fibrous smectite lining the inner walls followed by bladed to fibrous crystal aggregates of buff thomsonite 30-60 μm long of moderate birefringence. The amygdales are cored with massive blocky calcite (Fig. 6a). In 0larger amygdales and cavities, filling proceeds from the wall inwards with the sequence smectite-zeolites-calcite, forming comb-fill texture, ending with Fe-oxyhydroxides encrustation then quartz (Fig. 3e).

Some large, tens of centimeter wide corrosion vugs of irregular to elliptical shape are also incorporated within the volcano-sedimentary succession, specifically the lacustrine limestone (Fig. 6b). This limestone shows signs of metamorphism with recrystallized large crystals of calcite, graphite and garnet, as a result of thermal effect of the feeder basaltic dykes. The mineral assemblage of these vugs includes zeolites, illite, chlorite and Fe-oxyhydroxides. These large vugs infilling exhibit a rhythmic-zonal crystallization pattern from the wall inwards. The recrystallized calcite wall is followed by three well developed zeolite species arranged inwards as thomsonite, chabazite then natrolite (Figs. 6c). The thomsonite forms large spherules that are composed of up to 200 μm long, radially arranged fibrous crystals. The chabazite from blocky equant- squashed cubes and anhedral crystals that vary in size from

50 up to 300μm. Fan-like aggregates of acicular crystals of natrolite, up to 100 μm long, show epitaxial growth on the chabazite outwards into the calcite domains (Fig. 6c).The XRD patterns of the described vugs confirmed the presence of Ca-chabazite , natrolite and thomsonite (Fig. 6d).

Macroscopic whitish veins traverse the volcano-sedimentary succession (Fig. 6e), are occupied by a sequential crystallization of the mineral assemblage, zeolites, Fe-oxides, smectite, calcite and quartz. Chabazite is the only recorded zeolite; it forms an unusually large rossate form of euhedral bipyramidal crystals with a conspicuous penetrative twinning and inclusion-enhanced zoning ; the rims are inclusion-free (Figs. 6f & g).This is followed outward by a chalcedony zone that experiences a change in grain size from inner microcrystalline phase to small radiating fibrous one.

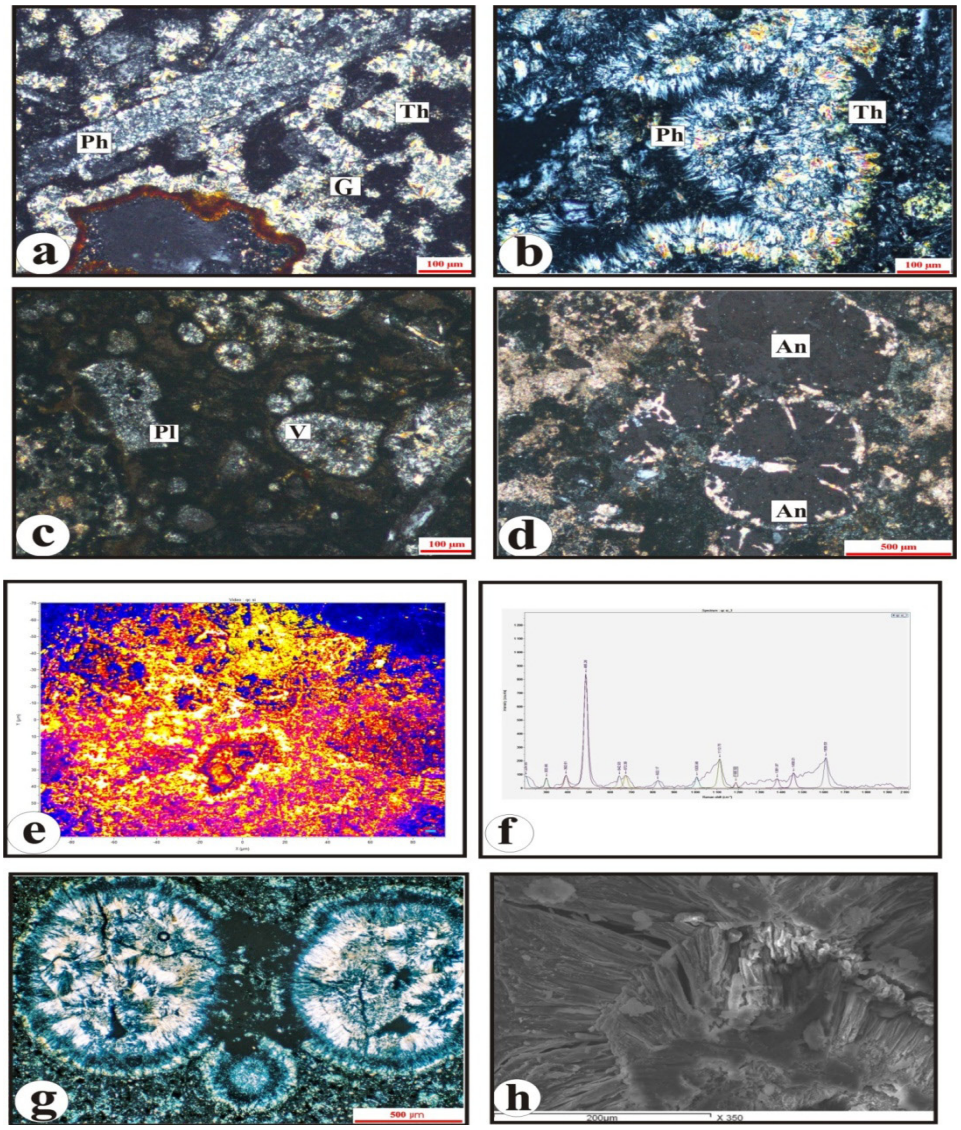

Fig. 5. a. Hyalocalstite tuff showing fibrous thomsonite nucleated along glassy remnants and growing into the interstitial spaces between the different components, note the presence of a large zeolitized plagioclase crystal fragment, CN. b. Rhythmic crystallization of fibrous phillipsite and thomsonite in the interstitial spaces of hyaloclastite tuff, CN. c. A large achnelithic fragment with numerous phillipsite-filled vesicles, hyaloclastite tuff, CN. d. Large rounded analcime (An) crystals rimmed and invaded by calcite (Ct) in tuffaceous matrix, lapilli tuff, CN. e. A Raman microscope imaging for an analcime crystal with invasion of late stage hydrothermal calcite f. Raman spectrum of the lapilli tuff showing the characteristic peaks of analcime. g: A fan-shaped fibrous tobermorite filling rounded vesicles that are lined by chlorite in glassy basalts, CN. h. A SEM-image of the tobermorite.

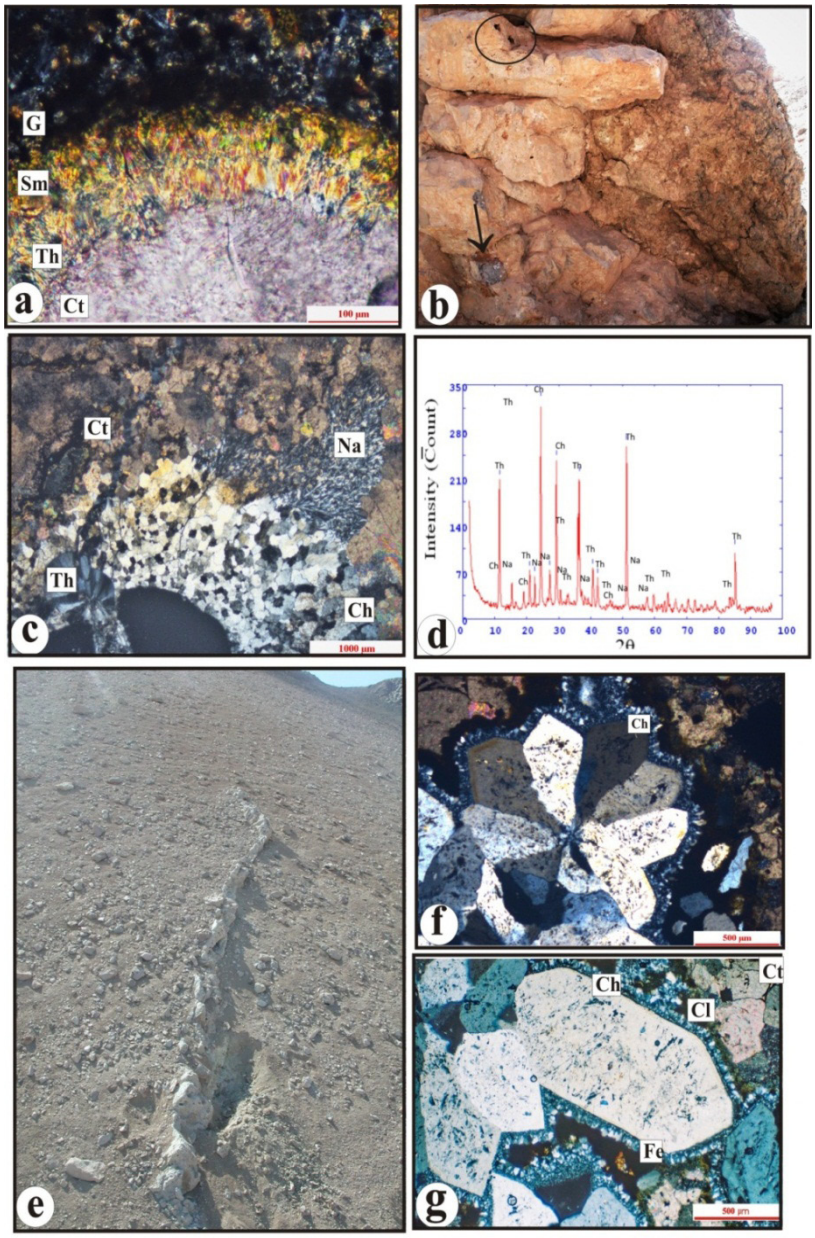

Fig. 6. a. A zonal arrangement of smectite-thomsonite-calcite filling a large rounded vesicle that is surrounded by a sheath of tachylite, scoriaceous basalt, CN. b: Elongated blocks of lacustrine limestone with numerous basaltic fragments (arrows) and corrosion vugs (circle). c: A corrosion vug filled with a sequence of thomsonite (Th)- chabazite(Ch)- natrolite(Na) minerals, CN. d: XRD- pattern of zeolites in one of the vugs showing the presence of thomsonite, chabazite-natrolite. e: A large whitish vein cutting the volcaniclastic rocks, W. Umm Thibua. f: A fracture filling large zoned rossate chabazite (Ch) crystal with penetrative twinning, CN. g: Euhedral bipyramidal crystals of chabazite rimmed by fibrous chalcedony, iron oxides then calcite.

Discussion and Conclusion

- The present work provides systematic mineralogical observations on the conditions and processes that prevailed during formation of different diagenetic and hydrothermal zeolite crystal generations of Abu Triefiya zeolite bearing volcaniclastic sequences. The concluded paragenetic sequences of the different zeolite mineral association and textural evolution during the diagenetic and hydrothermal processes are illustrated (Fig. 7).

Environment	Deposition	Diagenesis		Hydrothermal	Processes	
		Early	Late			
	Glassy basaltic clasts, basaltic glass & shards, pyrogenic mineral clasts, ash, mud.					
	mineral phase	**precursor**			**Texture type**	**Microscopic texture**
diagenetic mineral association	palagonite	sideromelane, glassy clasts			dissolution, replacement	selective-pervasive alteration
	smectite	palagonite			replacement, in-fill	selective alteration, pore-space, interclasts vesicles
	corrensite	smectite			replacement, in-fill	selective alteration, pore-space, interclasts vesicles
	chlorite	corrensite			replacement, in-fill	selective alteration, pore-space, interclasts vesicles,
	thomsonite I	plagioclase			replacement, in-fill	selective alteration, pore-spaces
	phillipsite	sideromelane, glassy clasts			in-fill	layered infill, pore-space, interclasts, vesicles
	analcime	palagonite			in-fill	equent, interclasts
	calcite					
hydrothermal mineral association	tobermorite			?	in-fill	layered infill, vesicles, spherulitic
	thomsonite II				in-fill	banded infill, fibrous, spherulitic
	chabazite				in-fill	banded in-fill massive
	natrolite				in-fill	banded in-fill fibrous
	calcite				in-fill	crustiform banding, comb-fill, massive in-fill, fracture
	quartz/chalcedony				in-fill	banded in fill , spherulitic
	gypsum	surficial subareal evaporation				

Fig. 7. Paragenetic sequences of the different zeolite mineral association and textural evolution during the diagenetic and hydrothermal processes.

- The volcaniclastic sequence in Abu Treifiya are mainly water-laid epiclastic deposits that exhibit signs of post depositional alteration processes affecting these units rich in volcanic glass. Most of the described zeolite crystal forms and textures are geometrically confined with certain volcaniclastic beds and facies and commonly arranged conformable to bedding and ascribed to diagenetic processes. Whereas post-diagenetic hydrothermal parageneses are related to fracture filling and dissolution vugs cross cutting the volcano-sedimentary bedding structure.

- The basaltic glass components exhibit different degrees of diagenetic alteration due to interaction with percolating aqueous solutions in the unconsolidated deposits. The diagenetic processes starts with alteration of volcanic glass which is a selective process involving hydration of glass and oxidation accompanied by extensive mobilization and leaching of Si^{4+}, $A1^{3+}$, Na^{+}, K^{+}, Ca^{2+} and Mg^{2+} ions to the medium (Stroncik and Schmincke, 2002). By increasing the pH and salinity of the pore fluids, clay minerals as smectite crystallize. On progression, the alkalinity

value reaches pH (~9-10) and salinity increase, conditions become favorable for crystallization of zeolites (Langella, *et al*., 2001, Snellings, *et al*., 2008;Weisenberger and Selbekk, 2009; McHenry, 2010; & Bastias, *et al*., 2016).The described alteration process and sequential formation of palagonite, clay minerals, zeolites and calcite is compatible with that commonly discussed by Hay and Iijima, (1968,a,b); Iijima and Harada (1969); Risso, *et al*. (2008) and Bastias, *et al*. (2016).

- Early diagenetic stage starts with formation of palagonite along margins of glass shards, basaltic clasts, and the included vesicles as rinds of yellow orange isotropic gel, followed by fibro-palagonite interlayered with smectite. Palagonite is considered as the main low temperature alteration product (<100^{o}C), during the lithification (post-deposition – early diagenesis) as concluded by Maicher et al. (2000); Drief and Schiffman (2004) & Dickinson et al.(2009). During the early diagenetic stage, smectite crystallizes on the expense of the palagonite, glassy basaltic clasts and shards, depositing along the internal vesicle wall- surfaces and in intergranular spaces. Smectite is occasionally followed by chlorite/ smectite (C/S) mixed layer with low chlorite content evolving to C/S with higher chlorite content to pure chlorite as microscopically recorded and confirmed by XRD in the hyaloclastite breccias and tuffs.
- The late stage of diagenesis involves the crystallization of different zeolite mineral generations. The zeolitization process is controlled by several conditions such as temperature, pressure, composition of the original rock and pore fluids as well as the prevailing physico-chemical conditions (pH and salinity). Precipitation of smectite increased the alkalis (Na^+ and K^+) ions in the solution and raised the pH that led to the deposition of phillipsite alone or accompanying thomsonite in varieties with high contents of plagioclase (probable source of Ca^{2+}), the commonest zeolites after smectite. Formation of phillipsite in lacustrine environments requires low Si activity (Honnorez, 1981; de′ Gennaro, *et al*. 1993, 1999 a, b; Johnson and Smellie, 2007). Phillipsite fibrous crystals rim glassy clasts, filling pore spaces and lining cavities creating a rather closed- system environment. Phillipsite is followed by the crystallization of analcime, depending on the evolution of the fluid composition. In areas around the lacustrine limestones, the pore fluids are suggested to be enriched in Ca^{2+} ions, which enhance the precipitation of fibrous calc- sodic thomsonite. In areas where the tuffs are surrounded by fluvial sandstones, the fluid composition is suggested to be becomes more sodic (increase of Na^+ ions) as the temperature and K^+ contents decrease promoting the crystallization of analcime. Formation of analcime as large spherical grains in lapilli and hyaloclastite tuffs indicate homogeneous nucleation at high degree of supersaturation in the more saline-alkaline fluids with low Si activity, similarly, concluded by Wilkin and Barnes (2000) and Do Campo, et al. (2007). Alt and Honnorez (1984) argued that celadonite precipitation (which increased the Na^+/K^+ ratio in solution) and decreased temperature (which favored Na^+ enrichment in the solution) may have contributed to analcime crystallization. Instead of celadonite as K^+ absorber, phillipsite played the same role in the studied rocks.
- The coexistence of these minerals might indicate a closed-basin of saline-alkaline lacustrine environments as well as fluctuation of physico-chemical conditions with the lake level, without a significant flux of cations entering or leaving the system (Gottardi, 1989; Snellings et al., 2008; McHenry, 2010). The compositional changes can be accounted for by a redistribution of elements present within the glass and the authigenic zeolite and clay minerals (McHenry, 2010). The studied zeolites (phillipsite, thomsonite and analcime) accommodate the Na^+, K^+ and Ca^{2+} whereas the Fe^{2+} and Mg^{2+} are hosted by smectite and chlorite, leaving the overall bulk composition with little changes. This diagenetic stage is also manifested by the progressive transformation of smectite with a the temperature stability of (100–200°, Dudoignon, *et al*., 1997), C/S mixed layer (200-230°C, Neuhoff, *et al*., 1999) to chlorite at around 240°C. This reflects the time and temperature-dependence of this transformation with depth of burial (*e.g*. Evards and Schiffman, 1983; Bettison and Schiffman, 1988; Bettison, *et al*., 1991; Weisenberger and Selbekk, 2009).
- The suggested diagenetic processes acquire surface waters percolate through fractures of the basalt flow and volcaniclastics, dissolving the glass and depositing clay minerals and

zeolites in regions close to the dissolution area.

- The hydrothermal open space zeolites which are mostly in the vicinity of the lacustrine limestones are characterized by larger size and number of zeolite species such as tobermorite, thomsonite-chabazite-natrolite, and chabazite alone, in amygdales, vugs and veins, respectively. The crystallization of large tobermorite spherules in some amygdaloidal basalt occurs mainly along the basalt-limestone contacts. Tobermorite is a hydrothermal metasomatic alteration product of calcium carbonate/basaltic rock interaction, where Ca^{2+} gained from the alteration of plagioclase and nearby limestone result in deposition of this calcic zeolite. The same conditions also prevailed in the formation of other calcic zeolites of the studied rocks. In the vugs, textural criteria indicate that thomsonite spherules formed first, then chabazite and natrolite. This occurs as a result of interaction between the glassy shards and fluids gaining the needed Na and Ca^{2+} from these fluids. With decreasing temperature and the evolution of the fluid composition with decreasing Si/Al ratio and increase the alkalinity Ca-chabazite is formed, then at much lower ratio, and increase in Na^{+} content fibrous natrolite crystallized. This association is indicative of low-T hydrothermal alteration (<100°C) as stated by Deer et al. (2004). The vein type-zeolites are related to the normal faults associated with the rift and recorded within the volcaniclastic rocks. It is monozeolitic with Na-chabazite that is accompanied with chalcedony, Fe-oxides, calcite, clays, and quartz. The high content of Na is probably related to the country rocks (i.e., hyaloclastites and associated peperite- hosted sandstones). The Na^{+}, K^{+}, Mg^{2+}, Ca^{2+} and Si^{4+} released during the palagonitization process form Na-chabazite, clays calcite and chalcedony. The effect of the host rock composition is best documented in the composition of chabazite, which is Ca-rich in the described vugs within the carbonate rocks and Na-rich in the veins. Additionally, Ca^{2+} ions can crystallize out of aqueous solution at much higher temperatures than Na and K, hence Ca-rich zeolites are crystallized first followed by the sodic varieties (Kotz and Purcell, 1987; Pe-Piper and Lisa Miller, 2002). As the temperatures of the hydrothermal solutions crystallizing the studied open spaced zeolites are not high enough for the Ca-rich zeolites as heulandite and laumontite to be crystallized, Ca-Na and Na- zeolites were formed. Finally, the studied zeolites have formed from alkaline hydrothermal solutions under low temperature and pressure conditions. The association of the diagenetic and hydrothermal zeolitization phases is probable as the temperature of the two models overlap around 100°C as reported by Gottardi (1989).
- In the studied rocks, the diagenetic model is applied for the zeolites in the volcaniclastic rocks as they are characterized by microcrystalline, fine fibrous phillipsite and thomsonite and later analcime for certain lithology, and differ compositionally and texturally from the larger and diverse hydrothermal zeolites in the later cross cutting open space filling.

Acknowledgments

The authors would like to deeply thank Prof. Dr. Mohamed El Sharkawi and Prof. Dr. Mortada El Aref for critical discussions. Prof. Dr. Ali Abdel Motelib - Prof. Dr. Abdel Hamid El Manawi for scientific advices. We greatly thank Prof. Dr. Mervat Hassan (Central Metallurgical R & D Institute) for XRD analysis and SEM and critical discussions during preparation of the text. Thanks, extend to Mr. Sameh El Tayyer (Faculty of Nanotechnology, Cairo University) for the Raman technique examinations. Deep thanks to our colleagues Prof. Dr. Osama Attia and Dr. Waleed Kassab for their beneficial discussions. The authors greatly thank the referees for their insightful and critical reading of the manuscript.

References

Abdel-Motelib, A. and Kabesh, M. (2014) Fossilized microbial and algal textures in post Eocene lacustrine zeolite tuff sequence, G. Abu Treifiya, Cairo- Suez Road, Egypt. ***5th*** *Conf. of the Inter. Symposium on Geography-Landscapes: Perception, Knowledge, Awareness, and Action*. Addleton Academic Publishers, New York: 163-174.

Abdel-Motelib, A., Kabesh, M., El Manawi A. and Said A. (2015) Oligocene lacustrine tuff facies, Abu Treifiya, Cairo-Suez Road, Egypt. *J. Afr. Earth Sci.*, **102** (2015), 33-40.

Abou Khadra, A. M., Wali, A. M. A., Müller, A. M. A., El Shazly, A. M. (1993) Facies development and sedimentary structures of syn-rift sediments,

Cairo–Suez District, Egypt. *Bull. Fac. Sci. Zagazig Univ.*, **15** (2): 355–373.

Abou Seda, A. A. (1980): The Volcanic Rocks of Gebel Abu Treifiya Area, Cairo–Suez District, Egypt. M. Sc. Thesis, Cairo Univ., 105 p.

Abou Seda, A. A. (2005): Mineral chemistry of the basaltic rocks of Gebel Abou Treifiya area, Cairo-Suez District, Egypt. In: Proceed. *Inter. Conf. on the Geology of the Tethys, 1st ed.,* Egypt, Cairo Univ., **1**, 124–133.

Alt, J. C., and Honnorez, J. (1984): Alteration of the upper oceanic crust, DSDP Site 417: mineralogy and chemistry. *Contrib. Mineral. Petrol.*, **87**: 149-169.

Bastias , J., Francisco Fuentes, Luis Aguirre, Francisco Hervé, Alain Demant, Deckart, K. and Torres, T. (2016) Very low-grade secondary minerals as indicators of palaeo-hydrothermal systems in the Upper Cretaceous volcanic succession of Hannah Point, Livingston Island, Antarctica . *Appl. Clay Sci.*, **134**, 246–256

Bettison, L. A., and Schiffman, P. (1988) Compositional and structural variations of phyllosilicates from the Point Sal ophiolite, California. *Am. Mineral.*, **73**, 62-76.

Bettison, L. A., Mackinnon, I. D. R. and Schiffman, P. (1991) Integrated TEM, XRD and electron microprobe investigation of mixed-layer chlorite smectite from the Point Sal ophiolite, California. *J. Metam. Geol.*, **9**: 697-710.

Cannata, C. B., De Rosa, R., Houghton, B., Donato, P. and Nudo, A. (2012) Pele's hair: case studies from Kilauea Volcano and Vulcanello (Aeolian Islands). *Acta Vulcanol. J. Nati. Volc.* Group of Italy, **23**/**24** 1/2.

Carracedo-Sánchez, M., Sarrionandia, F., Arostegui, J., Errandonea-Martin, J.,Gil-Ibarguchi, J. I. (2016) Petrography and geochemistry of achnelithic tephra from Las Herrerías Volcano (Calatrava volcanic field, Spain): Formation of nephelinitic achneliths and post-depositional glass alteration. *J. Volcanol. Geotherm. Res.* **327**: 484-502.

Cochemé, J., Aguirre, L., Bevins, R., Robinson, D. (1994) Zeolitization processes in basic lavas of the Báucarit Formation, northwestern Mexico. *Revista Geológia de Chile*., **21**, (2): 217-231.

Crovisier, J. L, Honnorez, J., Fritz ,B. and Petit, J. C. (1992) Dissolution of subglacial volcanic glasses from Iceland – laboratory study and modelling. *Appl. Geochem. Suppl.*, 55-81.

Deer, W.A., Howie, R.A., Wise, W.S., Zussman, J. (2004.) Volume 4B. Framework Silicates: Silica Minerals, Feldespathoids, and the Zeolites. *Geol. Soci.*, Rock-Forming Minerals, 48, London.

de′ Gennaro, M., Colella, C., Franco, E., Stanzione, D. (1988) Hydrothermal conversion of trachytic glass into zeolite. I. Reactions with deionized water: *Neu. Jahrb. Mineral Monat* **4**:149-158.

de′ Gennaro, M., Colella, C., Pansini, M. (1993) Hydrothermal conversion of trachytic glass into zeolite. 2. Reaction with high-salinity waters. *Neu. Jahrb. Mineral Monat* **3**:97-110.

de′ Gennaro, M., Incoronato, A., Mastrolorenzo, G., Adabbo, M., Spina, G. (1999a) Depositional mechanisms and alteration processes in different types of pyroclastic deposits from Campi Flegrei volcanic field (Southern Italy). *J. Volcanol. Geotherm. Res.* **91**:303-320.

de′ Gennaro, M., Langella, A., Cappelletti, P., Colella, C. (1999b) Hydrothermal conversion of trachytic glass to zeolite. 3. Monocationic model glasses. *Clays and Clay Min*. **47**:348-357.

de′ Gennaro, M., Cappelletti, P., Langella, A., Perrotta, A., Scarpati, C. (2000) Genesis of zeolites in the Neapolitan Yellow tuff: geological, volcanological and mineralogical evidence. *Contrib. Mineral. Petrol*. **139**: 17-35.

Dickinson, J.A., Harb N., Portner R. A. N.R. and Daczko N. R. (2009) Glassy fragmental rocks of Macquarie Island (Southern Ocean): Mechanism of formation and deposition. *Sed. Geol*. **216**: 91-103.

Do Campo, M., C. delPaPa, Jimenez-Millan and Nieto F. (2007) Clay mineral assemblages and analcime formation in a Paleogene fluvial-lacustrine sequence (Maiz Gordo Formation Paleogene) from northwestern Argentina. *Sed. Geol*. **201**, 56-74.

Drief, A., and Schiffman, P. (2004) Very low temperature alteration of sideromelane in hyaloclastites and hyalotuffs from Kilauea and Mauna Kea volcanoes: Implications for the mechanism of palagonite formation. *Clays and Clay Min*., **52**: 622–634.

Dudoignon, P., Proust, D. and Gachon, A. (1997) Hydrothermal alteration associated with rift zones at Fangataufa atoll (French Polynesia), *Bull. Volcan*. **58**, 583-596.

El Aref, M. M. (1984) Strata Bound and Stratiform Iron Sulfides, Sulfur, and Galena in the Miocene Evaporites, Ranga, Red Sea, Egypt (with special Emphasis on their Diagenetic Crystallization

Rhythmites). - In: Wauschkuhn, A. *et al*.: Syngenesis and Epigenesis in the Formation of Mineral Deposits. 457-467, **9**, Berlin - Heidelberg (Springer)

El Bayoumi, R., Hassanien, S. and Shallaly, N. A. (1998) The Tertiary basaltic rocks of Gabal Qatrani - the 6th. October City area. *GAW***4**, *Inter. Conf. Geol. the Arab World*, **1**, 287–299.

El Sharkawi, M. A. and Abu Khadra, A. M. (1968) The Dolerite-Limestone contact of Gebel Abu Treifiya, Cairo-Suez District. *J. Geol*., U.A.R.**12**(**1**),11-19.

Evards, R. C. and Schiffman, P. (1983) Submarine hydrothermal metamorphism of the Del Puerto ophiolite, California. *Am. J. Sci*., **283**, 289-340.

Farahat, E. S., Shaaban, M.M. and Abdel Aal, A. Y. (2007) Mafic xenoliths from Egyptian Tertiary basalts and their petrogenetic implications. *Gond. Res.*, **11**, **4**, 516-528.

Fontbotẽ, L. and Amstutz, G.C. (1980) New observations of diagenetic crystallization rhythmites in the carbonates facies of the Triassic of Alpujarrides (Betic Cordilera, Spain), comparison with other rhythmites. I Symp. Diagenesses, Barcelona, *Rev. Ist. Inv. Geol*., **34**: 293-310.

Gottardi, G. (1989) The genesis of zeolites. *Eur. J. Mineral*., **1**: 479-487.

Hay, R. L. and lijima, A. (1968a) Nature and origin of palagonite tuff; of the Honolulu Group on Oahu, Hawaii. *Geol. Soc. Am. Mere*.**116**:331 376.

Hay, R. L. and lijima, A. (1968b) Petrology of palagonite tuffs of Koko Craters, Oahu, Hawaii. *Contrib. Mineral. Petrol*., **17**: 141 154

Hay, R., Sheppard, R., (2001): Occurrence of zeolites in sedimentary rocks: An overview. In: D.L. Bish and D.W. Ming (eds.), Natural Zeolites: Occurrence, Properties, Applications. *Rev. Mineral. Geoch*., **45**, Washington, D.C., 217-234.

Honnorez, J. (1981) The aging of the oceanic crust at low temperature, in The Sea, edited by Emiliani, C., 525-587, John Wiley, Hoboken, N. J.

Iijima, A. and Harada, K. (1969) Authigenic zeolites in zeolitic palagonite tuffs on Oahu, Hawaii. *Am. Mineral*. **54**:182 197.

Johnson, J. S. and Smellie, L. (2007) Zeolite compositions as proxies for eruptive paleoenvironment, Geochem. Geophys. Geosyst., 8, Q03009, doi:10.1029/2006GC001450.

Khalaf, E. A., and Sano, T., (2020): Petrogenesis of Neogene polymagmatic suites at a monogenetic low−volume volcanic province, Bahariya depression, Western Desert, Egypt. *Int. J. Earth Sci.*,**109**, 995-1027.

Khalaf, E.A., Abdel Motelib, A. Hammed, M. S., El Manawi, A. (2015) Volcano-sedimentary characteristics in the Abu Treifiya Basin, Cairo–Suez District, Egypt: Example of dynamics and fluidization over sedimentary and volcaniclastic beds by emplacement of syn-volcanic basaltic rocks. *J. Volcanol. Geoth. Res.*, **292**, 1–28

Kotz, J. C. and Purcell, K. F. (1987) Chemistry and Chemical Reactivity. Saunders College Publishing, Montreal, 1020 p.

Langella, A., Cappelletti, P., and de'Gennaro, M. (2001): Zeolites in closed hydrologic systems. Pp. 235-260 in: Natural Zeolites: Occurrence, Properties, Applications (D.L. Bish and D.W. Ming, editors). *Reviews in Mineralogy and Geochemistry*, **45**, *Mineral. Soc. Am.,* Washington, D.C.

Maicher, D., White, J. D. L. and Batiza, R. (2000) Sheet hyaloclastite: density–current deposits of quench and bubble-burst fragments from thin, glassy sheet lava flows, Seamount Six, Eastern Pacific Ocean. *Mar. Geol*.**171** (1-4), 75-94.

McHenry,L. J. (2010) Element distribution between coexisting authigenic mineral phases in argillic and zeolitic altered tephra, Olduvai Gorge,Tanzania. *Clays and Clay Min.*, **58,** (5): 627-643.

Ming, D. W. and Allen, E. R. (2001) Use of natural zeolites in agronomy, horticulture, and environmental soil remediation, *Rev. Mineral. Geochem*., **45**: 619-654.

Mormone, A. and Piochi, M. (2020) Mineralogy, Geochemistry and Genesis of Zeolites in Cenozoic Pyroclastic Flows from the Asuni Area (Central Sardinia, Italy), *Minerals*, **10**, 268; doi:10.3390/ min10030268.

Neuhoff, P. S., Fridriksson T. and Arno´rsson S. (1999): Porosity evolution and mineral paragenesis during low-grade metamorphism of basaltic lavas at Teigarhorn, Eastern Iceland, *Am. J.Sci*. **299**: 467-501.

Neuhoff, P.S., Fridriksson, T. and Bird, D.K. (2000): Zeolite parageneses in the North Atlantic Igneous Provinces: implications for geotectonics and groundwater quality of basaltic crust. *Int. Geol. Rev*. **42**:15-44

Orlandi, P., and Scortecci, P.B. (1985): Minerals of the

Elba pegmatites, *Mineral. Rec*., **16**: 353-364.

Pansini, M. (1996) Natural zeolites as cation exchangers for environmental protection, *Miner. Depo*., **31**, 563-575.

Pe-Piper, G. and Miller, L. (2002) Zeolite minerals from the North Shore of the Minas Basin, Nova Scotia. *Atlantic Geol*. **38**, 11-28

Risso, C., Németh, K., Combina, A., Nulloa, F. and Drosina, M. (2008) The role of phreatomagmatism in a Plio-Pleistocene high-density scoria cone field: Llancanelo Volcanic Field (Mendoza), Argentina. *J. Volcanol. Geotherm. Res*., **169**: 61-86.

Said, R., (1990) The Geology of Egypt. Balkema, Rotterdam.

Shallaly, N. A., Beier, C., Haase, K. M. and Hammed, M. S. (2013) Petrology and geochemistry of the Tertiary Suez rift volcanism, Sinai, Egypt, *J. Volcanol. Geotherm. Res*., **267**:119–137.

Sheppard, R.A. and Hay, R. L. (2001) Formation of zeolites in open hydrologic systems. Pp. 261-275 in: Natural Zeolites: Occurrence, Properties, Applications (D.L. Bish and D.W. Ming, editors). Reviews in Mineralogy and Geochemistry, **45**, *Mineral. Soc. Am.,* Washington, D.C.

Snellings, R., Van Haren, T., Machiels, L., Mertens, G., Vandenberghe, N., and Elsen, J. (2008): Mineralogy, geochemistry, and diagenesis of clinoptilolite tuffs (Miocene) in the central Simav graben, western Turkey. *Clays and Clay Min*., **56**, 622-632.

Stroncik, N. A., and Schmincke H. U. (2001): Evolution of palagonite: Crystallization, chemical changes, and element budget. *Geochem. Geophys. Geosyst*., **2**, doi:10.1029/2000GC000102.

Stroncik, N. A. and Schmincke H. U. (2002) Palagonite A review, *Int. J. Earth Sci.,* **91**, 680-697.

Surdam , R. C. (1977): Zeolites in closed hydrologic system. *Rev. Mineral*, **4**:65-91.

Thorseth, I. H., Furnes, H. and Tumyr, O. (1991) A textural and chemical study of Icelandic palagonite of varied composition and its bearing on the mechanism of the glass-palagonite transformation. *Geochim. Cosmochim. Acta*, **55**:731-749.

Triana Juan Manuel R., Javier Francisco Herrera R., Carlos Alberto Rios R., Oscar Mauricio Castellanos A., Jose Antonio Henao M., Craig D. Williams and Clive L. Roberts (2012) Natural zeolites filling amygdales and veins in basalts from the British Tertiary Igneous Province on the Isle of Skye, Scotland, *Earth Sci. Res. SJ*. **16,** (1): 41-53.

Weisenberger, T. and Selbekk, R.S. (2008) Multi-stage zeolite facies mineralization in the Hvalfjördur area, Iceland. *Int. J. Earth Sci*., **98:** 985-999.

Weisenberger, T. and Selbekk, R.S. (2009) Multi-stage zeolite facies mineralization in the Hvalfjo¨rdur area, Iceland*. Int. J. Earth Sci*. (*Geol Rundsch*) **98**: 985-999.

Wilkin, R.T. and Barnes, H. L. (2000) Nucleation and growth kinetics of analcime from precursor Na-clinoptilolite. *Am. Mineral*. **85**, 1329-1341.

Utada M. (2001) Zeolites in Hydrothermally Altered Rocks. *Reviews in Mineralogy and Geochemistry* .**45** (1): 305–322.

أطوار نمو بلورات الزيوليت أثناء مراحل الطور التحويلي والطور الحراري المائي – دراسة للرواسب الفتاتية البركانية بحيرية التكوين، منطقة أبو طريفية، طريق القاهرة، السويس، مصر

مني كابش، ونهلة شلالي
قسم الجيولوجيا، كلية العلوم، جامعة القاهرة، جمهورية مصر العربية

تعتبر معادن الزيولايت والطين من المعادن الثانوية الشائعة في تتابع الصخور الرسوبية البركانية في حوض أبو طريفية. والتي يتم تشكيلها عن طريق تغيير التحلل المائي للزجاج البركاني عن طريق التفاعل مع الماء المتخلل في حوض مغلق جزئيًا لبيئة البحيرات المالحة والقلوية. تمت دراسة الزيوليت ومعادن الطين والكالسيت المصاحبة ووصفها بالتفصيل مجهريًا ومن خلال حيود الأشعة السينية، كما يتم أحيانًا تطبيق تقنيات المسح الإلكتروني الدقيق وتقنيات رامان. تم تسجيل ووصف الأنواع المعدنية الزيولايت من فيلبسايت وتومسونايت وتوبمورايت وتشبازيات وناترولايت وانالسيم. والتي تنتج عن تميه الزجاج البركاني في ثلاث مراحل من التكوين المعدني: ١) معادن الطين مثل السميكتايت والكلوريت / السميكتايت والكلوريت ، ٢) معادن الزيوليت، و٣) أخيرًا الكالسيت.

تشكلت هذه المعادن في مرحلتين متجاورتين: أ) طور التحويري، والتي تتمثل في تكوين معادن الطين ، تليها فيليبسايت أو تومسونايت ثم تتشكل بلورات الأناليسيم, وملء الفراغات البينية و الثقوب في معظم أنواع السطوح البركانية الرسوبية. وقد نتج هذا التتابع للمعادن نتيجة زيادة درجة الحموضة والقلوية وملوحة البيئة. و ب) الطور الحراري المائي الذي يمثله ملء الشقوق والجيوب في الصخور بالقرب من الحجر الجيري و يتجلى من خلال تكوين معادن غنية بالكالسيوم مثل توبرموريت. التومسونايت - التشبازايت الكلسى- ناترولايت نتيجة انخفاض درجة الحرارة وارتفاع في نسب الصوديوم . وكذلك التشبازايت الصودي ثم العقيق الأبيض هيدروكسيدالحديد ومعادن طينية.